Reply to reviews for 'The stability of present-day Antarctic grounding lines — Part B: Possible commitment of regional collapse under current climate.'

Reese, R., Garbe, J., Hill, E. A., Urruty, B., Naughten, K., Gagliardini, O., Durand, G., Gillet-Chaulet, F., Chandler, D., Langebroek, P. M., Winkelmann, R.

October 31, 2022

Reply to Anonymous Referee 2, https://doi.org/10.5194/tc-2022-105-RC2

Comments to Reese et al. (2022)
This study investigates the committed grounding line retreat due to MISI for the present-day climatic forcing. The MISI hypothesis states that the ice flux across the grounding line increases when the ice thickness increases and hence, when the grounding line retreats on a retrograde sloping bed, a positive feedback arises. The assessment of the grounding line retreat due to MISI is achieved by performing long-term runs (10,000 years) into the future. The reversibility is also tested by running the simulations for 20,000 years using a pre-industrial forcing.
The simulations use (optimized) melt rates from PICO and the historical climate forcing provided by ISMIP6 for the period 1850-2015 (the actual SMB forcing is only defined from 1950 onwards and is kept constant before). I believe it is an interesting study that looks at the slow equilibration time of the ice sheets and the long-term feedbacks involved with respect to the marine-based parts of the Antarctic ice sheet. Below you can find my suggestions to improve the manuscript.

We thank the reviewer for their support and reviewing our manuscript. We address all suggestions below.

During the review process we found that the temperature corrections applied during the PICO paremeter selection were too weak, i.e., the present-day melt rates were underestimated. We redid the parameter selection. The parameters are only marginally affected, but the temperature corrections changed. Based on this we then updated our ensemble. Doing so, we also changed the ensemble parameters and now focus on the most sensitive parameters from the previous ensemble (C_d and δ). This allows us to sample more values of the parameter δ and also include the 'min' and 'max' parameters for PICO. Doing so, we found 21 possible present-day configurations for the Antarctic Ice Sheet (called AIS1-AIS21). For all configurations, we redid the present-day continued and reversibility runs. We find that

our main conclusions are not affected by this. The main difference we find is that our states are more sensitive now, which is consistent with higher present-day melt rates, and reflected in all ensemble members showing long-term irreversible retreat of Thwaites and some now also showing retreat of Pine Island.

We are currently waiting for some simulations to finish before we can finalise the update of the manuscript that we will submit at a later stage. We reply to all comments below and provide the updated versions of the figures. Note that figures and tables reference to the numbers used here.

Main comments:
The manuscript shows that the main regions where the model parameters give grounding line retreat are the Amundsen Sea Embayment, the Filchner-Ronne Ice Shelf and the Ross Ice Shelf (along Siple Coast). In contrast to the observations, thinning is also identified along the Ross Ice Shelf and the Filcher-Ronne Ice Shelf in the simulations for the reference state. How realistic is the committed grounding line retreat in these regions when there is already a bias for the present day?

We agree that committed retreat in regions in which our historic simulations deviate from observed signals, as in FRIS and Ross, is not reliable. We thought about modifying the historic forcing to avoid such signals, but decided to record it as it is, since this is the ocean input we get from the CMIP5 model in combination with PICO that we decided to use. We changed Figure 4 (new version included below included as Fig. 1) by adding a label for the hatches in that figure to indicate regions in which observed and modelled present-day signals deviate substantially to hopefully make this more clear. We will add more discussion in the updated version of the manuscript (e.g., in the conclusions "Furthermore, we find retreat in the Siple Coast of Ross Ice Shelf and in Filchner-Ronne Ice Shelf under present-day climate that has to be considered with care as the pattern of mass changes in those regions is not in line with present-day observations. However, we can use this modelled retreat to test for reversibility, and we find that large-scale retreat of the grounding lines of Filchner-Ronne Ice Shelf and the Siple Coast of Ross Ice Shelf is reversible if they are allowed to regrow to their initial geometry.").

The modelled thinning rates in the Amundsen Sea Sector are rather low for the present day. To test for biases in the ocean forcing, a constant temperature anomaly is added to all ice shelves around the Antarctic. The Filchner-Ronne Ice Shelf and the Ross Ice Shelf are somewhat more closed off from oceanic heat, while the Amundsen Sea region might experience higher oceanic warming to match the observed thinning rates. Could it be more appropriate to apply a spatially variable ocean temperature anomaly to better match the observed thinning rates?

We agree that it would be an improvement to better match observed thinning rates. For this study, we decided to use the ISMIP6 forcing as it is rather than modifying it to improve the comparison of our model representation in present-day (e.g., removing the historic trend in the Weddell and Ross seas and increasing the trend in the Amundsen Sea). It would be interesting, as a next step, to think about why these issues arise. Note that with our new ensemble we did not apply these ad-hoc temperature sensitivity tests any more as we include different PICO parameters, which indirectly capture differences in melt rates between the historic and present-day states as the parameter sets have different sensitivities of sub-shelf melt rates to ocean temperature changes. Interestingly, also with the 'max' PICO param-

eters included in the ensemble which yield a higher increase in ocean-driven melt over the historic period as they start with lower melt rates in 1850, the modelled historic magnitude and pattern of mass loss was not substantially altered, see Fig. 2 and Table **??** *summarising the historic simulations.*

Specific comments:
L29: It makes more sense to me to report the regional warming around/above the Antarctic continent than the global mean.

Done.

L50: This is confusing, it sounds as if you use the present-day climate forcing to test for reversibility of the grounding line retreat. I guess not because on L66 you say that you use pre-industrial climate forcing for the reversibility simulations. Could you rephrase to make clear that the forward experiments include the present-day forcing?

We moved this sentence to the end of the paragraph, which reads now: "In this paper, we analyse the current trend in Antarctic grounding lines – observations show that they are clearly not in steady state at the moment – by investigating to which steady state positions grounding lines evolve towards under current climate conditions. To do so, constant present-day climate is applied in the simulations and no future changes in the climate conditions are included. This means that the simulations are not projections, but rather allow us to assess the commitment of grounding line retreat under continued current climate forcing. If we find that present-day climate conditions commit grounding lines to large-scale retreat, we test if this retreat was reversible under colder, pre-industrial climate.".

L306: Could you report the RMSE for ice thickness, ice-stream velocities, deviations in grounding and floating area and the differences between the ensemble members?

We will add this information in a new supplementary Table, below shown as Table 1.

L317: What is the rationale to look 10,000 years into the future? And why do you double the simulation time for the reverse experiments? On L372 you report that the ice sheet states evolve to a new equilibrium, but GL's might not have fully converged to a steady-state after 10,000 years.

We selected 10,000 years as a optimal value between computational time and duration of the simulation. For the reverse simulations we doubled the time to make sure that the states are really close to equilibrium as we found that readvance takes longer than retreat. With the 20,000 years we aim to exclude the possibility that the grounding line is reversible, but the model just did not run for long enough. We add this reasoning in the end of the section ("To test if the grounding line positions attained after 10,000 years are reversible to their current state, we revert the climate forcing back to the 1850-conditions. We then run those simulations for another 20,000 years with constant historic (1850) climate. We reverse the simulations for twice as long to make sure that no readvance occurs which was found to take longer than retreat."). The full equilibrium state is usually not fully reached after 10,000 years, but since we are primarily interested in large-scale retreat, we think that this time period is sufficient to understand the large-scale patterns. To obtain proper steady states, we would probably need to run the model for 100,000 year time scales. In former line 372, we add "Note that 10,000 years might not be sufficient to reach a full equilibrium, but we

get a clear indication of what such an equilibrium state might look like." to make clearer that the ice sheet evolves towards *a steady state.*

L347: The sentence 'This as well as the choice of the sliding law, has been found also in previous studies' looks incomplete.

Thanks. We will add the missing piece.

L367: You report the model drift during the historical simulations, but what is the model drift during the next 10,000 years?

To discuss this, we add the model drift over the next 10,000 years in a Table of the new manuscript (below given as Table 2 which is a combination of the previous Tables 2,3,4) and report the mass loss there now relative to the model drift.

L379: The ensemble members indicating substantial grounding line retreat occur for more slippery bed conditions or higher oceanic temperatures. Hence making the model more sensitive increases the chances that the tipping point is reached. Low values for the till effective overburden fraction strongly enhance the grounding line retreat. Could you add a word on the likelihood for the model parameter choices made?

There are three studies that allow us to put an estimate on δ. Engelhardt and Kamb (1997) and Smith et al. (2021) performed measurements in boreholes of Whillans and Rutford ice streams, respectively. They estimate values for the effective pressure in the drainage system ($N = P_0 - P_w$ with ice overburden pressure $P_0 = \rho_i g h$ and subglacial drainage system water pressure P_w.). Those values are found to be within $0.7 \pm 0.7\%$ of the ice overburden pressure. Although the pore water pressure in the till P_{till} is different from the subglacial drainage system water pressure P_w, since the systems are connected and the water pressure must be continuous at the interface between water and till, those values above yield an upper bound on δ (which is the fraction of the effective pressure in the till to the ice overburden pressure). A direct estimate of Blankenship et al. (1987) yields a value of $\delta \approx 0.006$. We will add this discussion to the manuscript.

Figure 6: Put a box around the figures to increase clarity, maybe add names for the ice shelves to make it more clear for the reader what we are looking at.

We updated this figure (below as Fig. 4). Since more ensemble members show large-scale retreat now, we only show a selection of runs in this figure and will create an additional figure with reversibility plots for all members and add it to the supplement. We will update the discussion on reversibility accordingly.

References

Blankenship, D. D., Bentley, C. R., Rooney, S., and Alley, R. B.: Till beneath Ice Stream B: 1. Properties derived from seismic travel times, Journal of Geophysical Research: Solid Earth, 92, 8903–8911, 1987.

Engelhardt, H. and Kamb, B.: Basal hydraulic system of a West Antarctic ice stream: constraints from borehole observations, Journal of Glaciology, 43, 207–230, 1997.

Morlighem, M., Rignot, E., Binder, T., Blankenship, D., Drews, R., Eagles, G., Eisen, O., Ferraccioli, F., Forsberg, R., Fretwell, P., et al.: Deep glacial troughs and stabilizing ridges unveiled beneath the margins of the Antarctic ice sheet, Nature Geoscience, 13, 132–137, 2020.

Shepherd, A., Ivins, E., Rignot, E., Smith, B., Van Den Broeke, M., Velicogna, I., Whitehouse, P., Briggs, K., Joughin, I., Krinner, G., et al.: Mass balance of the Antarctic Ice Sheet from 1992 to 2017, Nature, 558, 219–222, 2018.

Smith, A., Anker, P., Nicholls, K., Makinson, K., Murray, T., Rios-Costas, S., Brisbourne, A., Hodgson, D., Schlegel, R., and Anandakrishnan, S.: Ice stream subglacial access for ice-sheet history and fast ice flow: the BEAMISH Project on Rutford Ice Stream, West Antarctica and initial results on basal conditions, Annals of Glaciology, 62, 203–211, 2021.

Table 1: Summary of ensemble indicators. RMSE stands for root-mean-square deviation in ice thickness (h) or ice stream velocities (v) to present-day observations. We further test for deviations in grounded and floating area, and the average distance to the observed grounding line position. We calculate the average rate of ice thickness change. The last dimension is the difference to observed sea-level trend. We lay a specific focus on the Amundsen region (ASE), Filchner-Ronne (FRIS) and Ross (RIS) ice shelves by additionally evaluating each indicator for these drainage basins individually.

indicator	AIS1	AIS2	AIS3	AIS4	AIS5	AIS6	AIS7	AIS8	AIS9	AIS10	AIS11	AIS12	AIS13	AIS14	AIS15	AIS16	AIS17	AIS18	AIS19	AIS20	AIS21
RMSE(h)$_{AIS}$ (m)	335.65	344.50	349.50	347.75	348.02	347.63	345.03	344.92	348.71	345.37	341.46	343.40	345.89	344.49	343.37	342.85	341.65	340.92	343.83	343.65	342.37
RMSE(h)$_{ASE}$ (m)	172.62	182.90	192.72	182.70	191.34	187.77	173.75	185.03	194.93	185.39	167.93	193.79	184.16	191.74	184.16	199.80	185.60	203.30	201.87	197.09	221.61
RMSE(h)$_{RIS}$ (m)	268.56	276.04	286.65	281.10	275.89	286.01	268.20	268.99	271.40	265.43	264.46	267.27	263.32	263.58	256.77	262.12	257.55	257.86	261.68	257.62	256.24
RMSE(h)$_{FRIS}$ (m)	240.53	247.34	256.51	242.43	249.94	253.41	241.91	240.85	256.63	248.36	226.36	242.13	236.00	236.04	235.60	244.13	228.03	238.00	228.89	225.56	228.62
RMSE(v)$_{AIS}$ (m/a)	257.61	250.28	247.51	263.44	250.92	252.23	276.08	249.11	244.55	253.32	297.70	260.78	275.21	272.92	272.29	247.34	305.83	255.27	275.49	306.04	299.63
RMSE(v)$_{ASE}$ (m/a)	74.84	68.47	69.46	67.66	68.52	65.51	80.71	72.32	68.32	75.41	100.74	72.72	94.67	87.11	85.68	77.92	122.60	95.78	98.00	127.17	147.09
RMSE(v)$_{RIS}$ (m/a)	33.39	31.86	33.32	33.28	34.56	32.97	36.33	32.64	34.83	33.71	36.67	40.23	33.01	34.82	38.26	37.18	36.40	34.47	35.92	37.22	35.13
RMSE(v)$_{FRIS}$ (m/a)	24.19	23.49	22.60	23.34	22.83	22.46	23.67	23.35	22.82	24.33	25.19	23.91	23.58	23.69	25.19	23.67	24.78	24.57	24.39	24.67	25.36
ΔA^g_{AIS} (km^2)	685440	693504	706880	695040	718016	707136	690368	713088	729664	722368	671296	726336	709376	721152	713600	731648	680128	727872	710464	698752	712704
ΔA^g_{ASE} (km^2)	8512	8192	7104	7936	8128	7808	8704	9088	8256	9152	10112	10496	10112	11072	10432	11648	12800	15232	14976	15168	19072
ΔA^g_{RIS} (km^2)	128256	123904	125312	127552	134656	128256	125376	140096	135744	137728	132160	153024	144128	153856	143552	151360	130240	154368	155520	145856	155776
ΔA^g_{FRIS} (km^2)	109056	114496	119808	106816	113664	116864	111744	106240	119616	116992	97664	105216	102400	102016	107136	109312	102016	106688	96256	98176	99648
ΔA^f_{AIS} (km^2)	567296	578816	592192	576064	588544	587904	577600	582400	601280	592000	558592	600768	580928	598976	584896	605312	568384	602688	585472	570048	587584
ΔA^f_{ASE} (km^2)	8896	9792	9472	9408	13312	9664	10048	11200	13184	11264	11008	14976	12800	16704	12800	16320	13440	18176	17472	15552	21440
ΔA^f_{RIS} (km^2)	85760	81152	82432	84992	92288	85632	82880	97856	93248	95360	89664	111040	101888	112192	101184	109248	87680	112192	113920	103680	113728
ΔA^f_{FRIS} (km^2)	97344	102656	107776	94976	101824	105088	99584	94272	107776	105216	85760	93376	90432	90368	94976	97536	89984	95104	84416	86336	87744
ΔGL_{AIS} (km)	9.47	9.78	9.76	10.24	10.27	10.03	9.82	10.56	10.54	10.27	9.82	11.18	10.66	11.20	10.70	11.13	10.14	11.43	11.05	10.59	11.16
ΔGL_{ASE} (km)	6.67	7.05	6.83	6.47	6.02	6.43	6.70	6.90	6.03	7.09	8.56	8.21	8.45	9.56	8.23	9.66	11.16	14.67	13.80	13.00	18.01
ΔGL_{RIS} (km)	21.40	19.76	19.91	21.22	23.89	21.00	20.20	25.64	24.23	24.73	23.15	29.63	27.65	30.56	26.69	29.41	22.93	30.54	31.26	28.34	31.32
ΔGL_{FRIS} (km)	12.47	13.63	13.36	14.91	13.84	13.55	13.22	15.01	14.38	12.49	12.92	14.93	14.23	13.95	14.50	14.74	13.96	14.32	13.12	13.01	13.67
dhdt$_{AIS}$(mm/a)	83.70	86.64	83.01	86.30	69.36	81.55	87.13	71.76	69.35	72.12	91.51	62.82	76.11	64.79	79.10	62.28	96.45	63.76	64.64	80.96	71.86
dhdt$_{ASE}$(mm/a)	95.57	99.81	93.98	91.59	71.98	105.42	97.27	76.76	67.36	89.45	124.36	77.03	101.71	89.79	102.01	86.84	143.86	70.09	82.65	125.65	139.86
dhdt$_{RIS}$(mm/a)	43.14	42.35	40.16	44.47	34.15	40.46	44.35	35.98	37.26	34.72	45.03	30.73	35.26	28.63	37.82	29.95	44.92	29.80	31.75	37.92	31.38
dhdt$_{FRIS}$(mm/a)	39.16	37.64	39.82	40.65	33.84	39.04	38.91	35.34	32.98	32.42	39.17	27.59	34.90	26.97	34.38	27.35	39.62	27.14	27.35	34.24	28.36
Δ SLE (mm)	6.25	5.71	6.22	6.17	8.10	6.73	5.96	7.39	7.96	8.13	5.16	8.88	7.45	7.50	6.47	9.00	2.79	7.65	8.57	5.67	6.93

Table 2: PISM parameters of the 21 ensemble members and modelled mass changes. Runs are sorted starting with the best scores shown in Fig. 3. Given are modelled mass changes between 1992 and 2015, between 1850 and 2015 (both relative to the control run), and drift in the control run between 1850 and 2015 in mm SLE for all ensemble members. This can be compared to observed mass loss of 7.6 $\pm$ 3.9 mm SLE between 1992 and 2017 (Shepherd et al., 2018). Furthermore, we summarise committed mass loss after 10,000 years, relative to the control run, and the drift in the corresponding control run (in m SLE). Positive numbers indicate mass gain, negative mass loss.

	δ (%)	C_d (mm/a)	PICO	$\Delta V_{2015-1850}$ (mm SLE)	$\Delta V_{2015-1992}$ (mm SLE)	$\Delta V_{CTRL,2015-1850}$ (mm SLE)	$\Delta V_{12,015-2015}$ (m SLE)	$\Delta V_{CTRL,12,015-2015}$ (m SLE)
AIS1	1.75	10	max	-7.35	-0.49	-7.03	-3.41	-0.22
AIS2	2.00	7	max	-10.06	-0.99	-5.02	-3.47	-0.17
AIS3	2.25	7	max	-5.44	-0.50	-4.28	-3.48	-0.19
AIS4	2.00	10	max	-6.39	-0.67	-5.45	-3.32	-0.23
AIS5	2.25	10	best	-1.88	1.39	-5.71	-3.17	-0.22
AIS6	2.25	10	max	-3.32	0.07	-7.00	-3.34	-0.23
AIS7	1.75	7	max	-7.54	-0.85	-5.96	-3.19	-0.20
AIS8	2.00	10	best	-3.56	0.67	-5.45	-3.10	-0.21
AIS9	2.25	7	best	-1.94	1.29	-5.30	-3.17	-0.21
AIS10	2.00	7	best	-1.61	1.32	-4.81	-2.93	-0.19
AIS11	1.50	10	max	-8.28	-1.54	-4.27	-3.25	-0.23
AIS12	2.25	10	min	-0.38	2.13	-5.47	-2.79	-0.22
AIS13	1.75	10	best	-3.35	0.66	-5.88	-3.00	-0.21
AIS14	2.00	10	min	-3.48	0.81	-4.58	-2.65	-0.26
AIS15	1.75	7	best	-8.17	-0.32	-5.54	-2.87	-0.19
AIS16	2.25	7	min	0.04	2.26	-2.90	-2.78	-0.20
AIS17	1.50	7	max	-13.39	-3.99	-4.30	-3.13	-0.19
AIS18	2.00	7	min	-3.57	0.92	-5.02	-2.52	-0.22
AIS19	1.75	10	min	-1.56	1.81	-4.67	-2.58	-0.22
AIS20	1.50	10	best	-8.53	-1.16	-3.90	-2.98	-0.23
AIS21	1.75	7	min	-5.65	0.07	-7.81	-2.60	-0.23

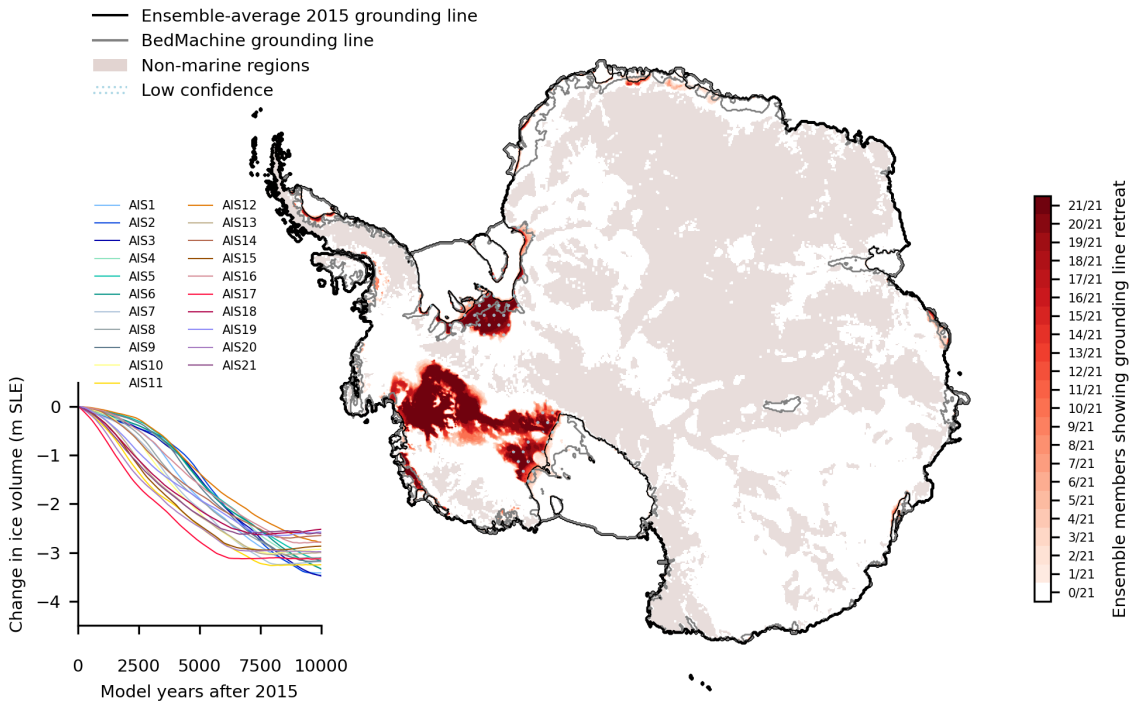

Figure 1: **Long-term evolution of present-day Antarctic grounding lines under constant present-day climate conditions.** Starting in present-day after the historic forcing from 1850 to 2015, simulations are continued with constant present-day climate for 10,000 years. Red colors show regions over which the grounding line retreats. The darker the red, the more simulations show grounding line retreat over the respective region in the different simulations corresponding to variations in basal sliding and ice flow parameters (retreat is plotted in comparison to a control simulation). Black contour shows ensemble-average initial grounding line position in 2015. Inset shows the evolution of sea-level relevant ice volume for all ensemble members (m SLE, metres sea-level equivalent, relative to the drift in the initial state over that period). Dots on retreat areas indicate regions in which present-day modelled thinning deviates from observations (namely for Filchner-Ronne and Ross ice shelves). Light brown indicates bedrock above sea level, white areas indicate bedrock below sea level. Note that retreat occurs only in marine regions which have bedrock below sea level.

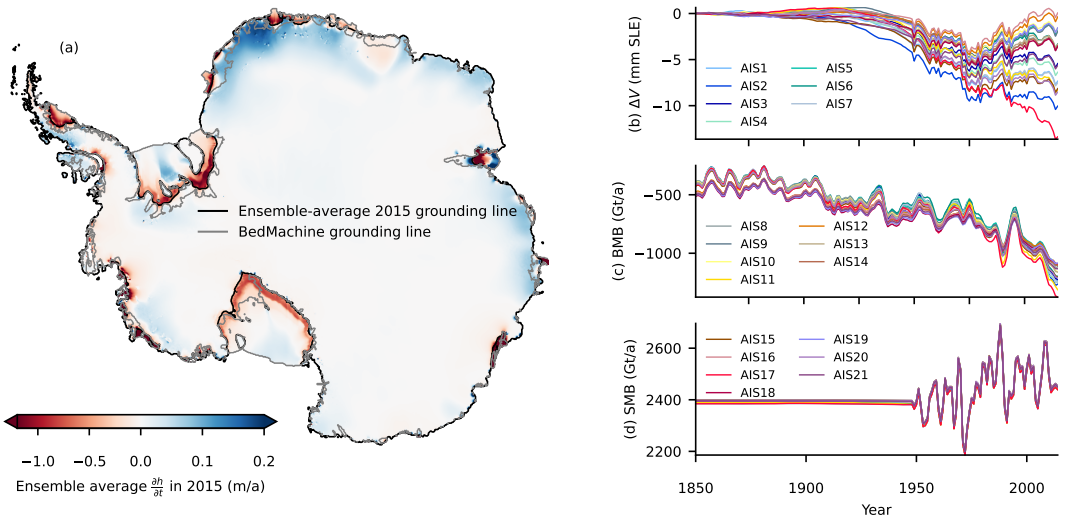

Figure 2: **Historic simulations from 1850 to 2015 and present-day ice sheet configurations.** Shown are (a) ensemble-average rates of ice thickness changes in 2015 (relative to control) with average grounding line position, and evolution of (b) the sea-level relevant ice volume (in millimetres sea-level equivalent, mm SLE), (c) basal mass balance of ice shelves (excluding melting in grounded regions), and (d) surface mass balance (both in gigatons per year).

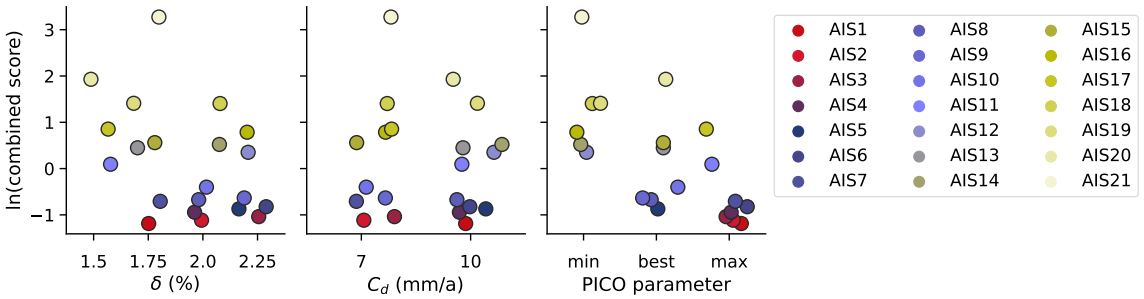

Figure 3: Scoring of ensemble of initial configurations in 2015. Scores are based on observed ice thickness, velocities, mass loss, grounding line positions, and a special focus is given to the Amundsen, Ross and Weddell seas. Initial ensemble members were obtained from equilibrium simulations of a full parameter ensemble with all runs that showed grounding lines broadly in agreement with present-day continued after 5000 to full 25,000 years (total of 21 runs). For each a historic simulation was run from 1850 to 2015. The 2015 state is then scored with present-day observations. Shown is the natural logarithm of the scores. The lower the values the better the agreement with present-day.

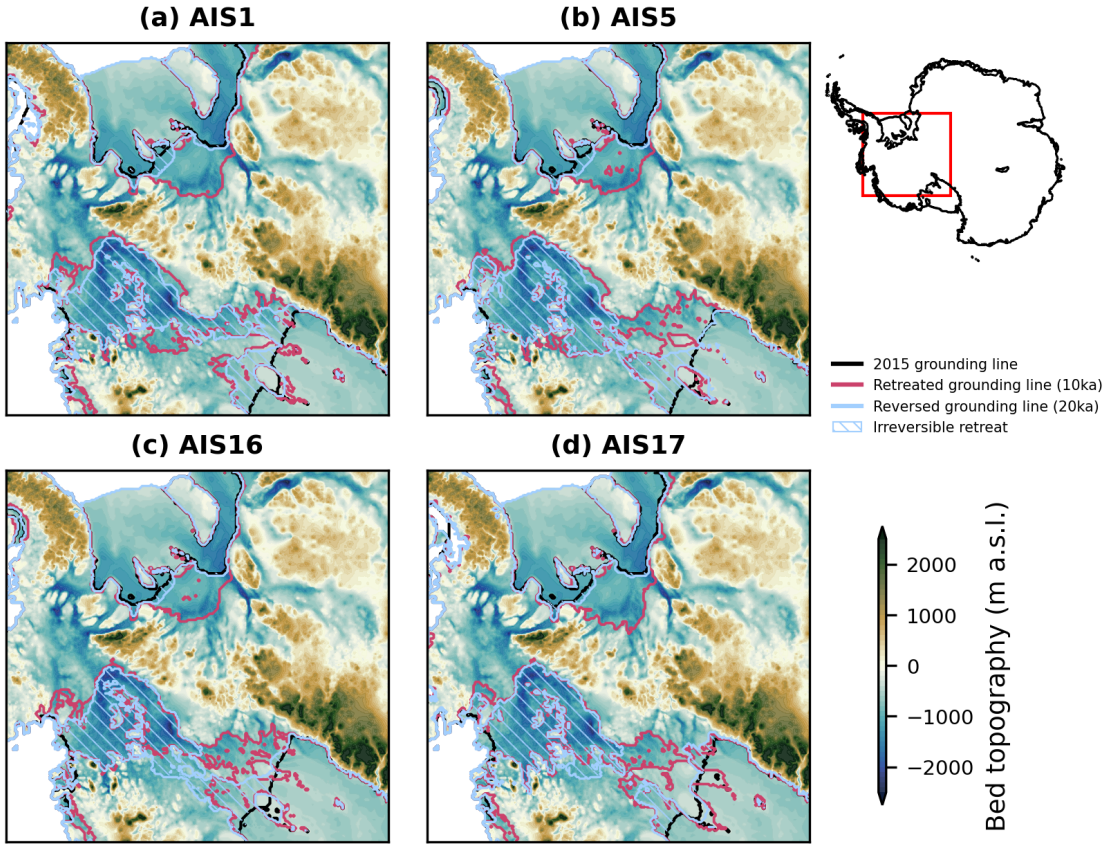

Figure 4: **Reversibility experiments of large-scale retreat in West Antarctica.** Four present-day configurations of West Antarctica, with their 2015 grounding lines shown in black, show large-scale retreat under constant present-day climate (red lines show grounding line positions after 10,000 years), see also Fig. 1. When reversing the climate to historic conditions for 20,000 years, the grounding lines evolve to the positions shown in blue. The blue hatches show areas over which grounding lines are not reversible. The spatial map shows the bed topography from Bedmachine (Morlighem et al., 2020). We here show the best ensemble member (AIS1), the best ensemble member for 'mean' PICO parameters (AIS5), the least sensitive member, i.e., with most mass gains between 1992 and 2015 (AIS15), and the most sensitive member, i.e, with most mass loss between 1992 and 2015 (AIS16). Inset shows the map location in Antarctica.